devices based on epitaxial yttrium iron garnet," *Proc. IEEE.* vol. 64, no. 5, pp. 794–800, 1976.
[3] N. D. J. Miller, "Magnetostatic volume wave propagation in a dielectric layered structure," *Phys. Stat. Sol. (a)*, vol. 37, pp. 83–91, 1976.
[4] Z. M. Bardai, J. D. Adam, J. H. Collins, and J. P. Parekh, "Delay lines based on magnetostatic volume waves in epitaxial YIG," *AIP Conf. Proc.* no. 34, pp. 268–270, 1976.
[5] N. S. Kapany and J. J. Burke, *Optical Waveguides*. New York, Academic, 1972.
[6] M. S. Sodha, G. D. Gautama, and A. K. Chakravarty, "Propagation of optical pulses through claded fibers: Modified theory," *Appl. Optics*, vol. 12, pp. 2482–2485, 1973.
[7] H. Kogelnik and H. P. Weber, "Rays, stored energy and power flow in dielectric waveguides," *J. Opt. Soc. Amer.*, vol. 64, pp. 174–185, 1974.
[8] P. K. Tien, "Integrated optics and new wave phenomena in optical waveguides," *Rev. Mod. Phys.*, vol. 49, pp. 361–420, 1977.
[9] V. Ramaswamy, "Ray model of energy and power flow in anisotropic film waveguides," *J. Opt. Soc. Amer.*, vol. 64, pp. 1313–1320, 1974.
[10] L. Brillouin, *Wave Propagation and Group Velocity*, New York: Academic, 1960.
[11] N. C. Srivastava, "Non-reciprocal reflection of Electromagnetic waves from magnetized ferrite," *J. Appl. Phys.*, vol. 49, pp. 3181–3189, 1978.
[12] L. M. Brekhoskikh, *Waves in Layered Media.* New York: Academic 1960, p. 104.
[13] S. S. Gupta and N. C. Srivastava, "Power flow and energy distribution of magnetostatic bulk waves in a dielectric layered structure," *J. Appl. Phys.*, 1979.
[14] R. H. Randard, "Total reflection: A new evaluation of the Goos-Hanchen shift," *J. Opt. Soc. Amer.*, vol. 54, pp. 1190–1197, 1964.
[15] S. S. Gupta and N. C. Srivastava, "Physics of microwave reflection at a dielectric-ferrite interface," *Phys. Rev. B*, vol. 19, pp. 5403–5412, 1979.

Surface Electromagnetic Wave Field Strength Measurements on Railroad Tracks

BRIAN C. H. LAI AND CHARLES A. GOBEN, MEMBER, IEEE

Abstract—**This paper reports an experimental investigation of surface electromagnetic wave (SEW) energy distribution on railroad tracks. Radial field distribution of SEW on 112-lb/yd rails were examined utilizing a dipole diode detector. Laboratory and on site measurements were made. The field strength distribution data at frequencies 3.000, 6.000, and 9.733 GHz show that the main part of the SEW TE mode energy (almost 90 percent) is on the head of the rail. Use of dielectric augmentation on the side of rails resulted in lower attenuation of the propagating SEW. Thick dielectric strip augmentation data shows enhancement of SEW propagation in agreement with McAulay. The intertrack coupling and the characteristic frequency response versus field strength at varied distances from the source were also examined. These data indicate propagation distances of more than 2000 m are possible using dielectric augmentation.**

I. Introduction

OBSTACLE detection and communication for high-speed railroad systems have been playing an increasingly important role in railroad system performance. Automation can contribute to economical operation in such systems. Surface electromagnetic wave (SEW) excitation techniques and their applications have been considered in many papers which involve the United States, United Kingdom, Japan, and Canada. One such microwave communication system for centralized train traffic control utilized the TE_{01} mode propagating within a circular waveguide [1]. The use of guided high-frequency electromagnetic waves transmitted parallel to the railway track for the purpose of providing radar location of trains as well as continuous telephonic communication with drivers and guards on the trains has been developed by the Britich [2]. In Japan, a metallic waveguide with periodic teeth ("Corrugated-Y-Guide") and a radar set have been developed for a moving block system and obstacle detection in high-speed railways [3],[4]. A Sommerfeld Goubau wave propagated on the surface of a *G* line may also be used for train and obstacle detection [5].

Currently, there is a strong interest in surface electromagnetic waves utilizing several SEW excitation techniques [6]–[9]. One attempt to minimize the vast inventory on the system is to adapt the track for use as an open waveguide [9]. A prism coupler which has no physical contact with the rail was designed in order to excite and detect surface electromagnetic signals from the train. The field patterns are needed to assist in the design of suitable antennas for coupling the appropriate mode in and out of the wave guide in order to utilize the prism coupling technique [8] in an application to collision avoidance [9].

Manuscript received November 4, 1979; revised February 26, 1980. This work was supported in part by the U.S. Department of Transportation under Contracts DOT-TSC-1150-Goben and DOT-TSC-1217-Goben.

B. C. N. Lai was with the Engineering Research Laboratory, University of Missouri-Rolla, Rolla, MO 94070. He is now with the Communications Transistor Corporation, Varian Associates, San Carlos, CA 94070.

C. A. Goben is with the Department of Electrical Engineering and the Engineering Research Laboratory, University of Missouri-Rolla, Rolla, MO 65401.

0018-9480/80/0800-0919$00.75 ©1980 IEEE

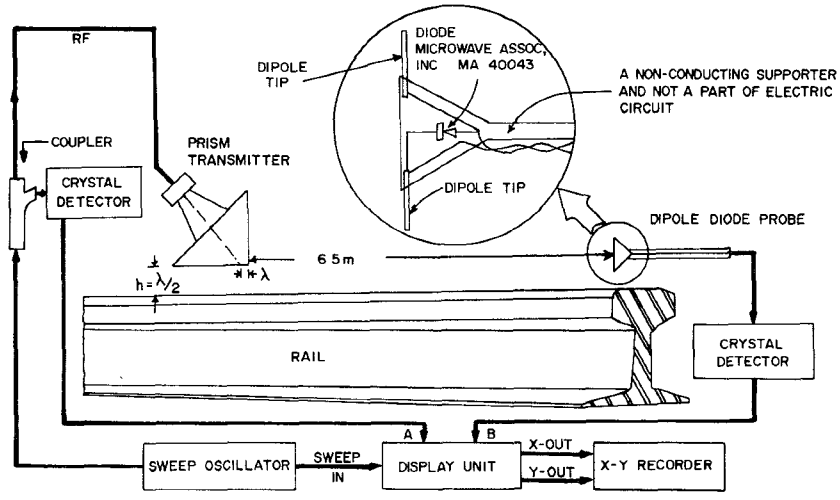

Fig. 1. Experimental setup for radial field strength distribution measurement using dipole diode probe method to measure reliable data at one centimeter intervals around the rail cross section.

It has been reported that it is theoretically possible to enhance SEW propagation by coupling to thick dielectric strips on the side of the rail by McAulay [10]. He adapted an analytical (or numerical) method to analyze waveguides of arbitrary shape and arbitrary dissipative materials. His computer numerical calculations assumed that a large fraction of the SEW propagates along the rail–dielectric interface. The interface between the dielectric medium and the air provides the coupling between the TM and TE modes which enables hybrid modes to propagate along the dielectric–metal interface.

The first part of this paper reports an experimental investigation of SEW energy distribution on railroad rails. The field strength of the SEW was detected by using a dipole microwave diode probe and assuming the wave has a TE mode configuration. It is essential to understand the field distribution around the rail periphery if suitable antennas are to be designed for coupling the appropriate mode into and out of the waveguides. Attenuation of the field must be kept to a minimum to improve SEW signal propagation and to ensure detection of trains and obstacles on the track at long ranges.

The latter part of this paper reports an experimental investigation of SEW with dielectric augmentation on the sides of rails. It was found that augmentation lowers the attenuation of the propagating SEW. The frequency response versus field strength at various distances from the source was also examined. Experiments were conducted using a prism coupler source to couple the electromagnetic energy to the surface of the rail. The lowest order mode which propagates is similar to the TE_{11} mode on a dielectric strip. In this case the transverse electric field through the dielectric is approximately vertical.

II. Experiments

A. Radial Field Distribution of SEW on Rail Tracks Measured by a Dipole Diode Probe Detector

The experimental setup for the radial field distribution measurement utilized the dipole diode probe as shown in Fig. 1. A SEW was excited on the rail using a prism coupler [6]–[8] positioned a half-wavelength above the rail head surface. The transmitting horn antenna was fastened on the prism and the whole coupling assembly was shielded with microwave absorbing material to eliminate stray radiation [7],[8]. At the receiving point, the propagated SEW was detected by the receiving antenna with a dipole microwave diode probe and displayed. Laboratory and on-site measurements were made. The dipole microwave diode probe detector was employed to obtain data at 1-cm intervals around the rail cross section. The probe was composed of a microwave diode connected between a half-wave length dipole at the frequency of interest as shown in the circle insert in Fig. 1. The dipole tip is positioned normal to the rail surface in order to satisfy the boundary condition which states that $\bar{E}$ is normal to the surface of the rail. Then the measurements of electric field strength by the probe were made at a distance of $\lambda/2$ from the rail and at 1-cm intervals along the outer rail periphery.

Fig. 2 shows the radial field strength distribution (near field) as a function of distance from the rail center, around the rail cross section at 3.000 GHz, 6.000 GHz, and 9.733 GHz.

The inset of the rail profile in Fig. 2 shows how the distance (in centimeters) from the rail head center was measured. One can see that the field strength at 9.733 GHz has a larger distribution on the rail flat top surface than at the other two frequencies. The data at 3.000 and 6.000 GHz indicate a higher radial field distribution on both sides of the rail. The relatively high distribution at the rail flange is a typical phenomenon for an indoor measurement since the laboratory rail setup excluded joint bars and the rails were blocked 20 cm above the laboratory floor. The data shows that the main part of the SEW energy (almost 90 percent) is on the head of the rail, i.e., the range between -6.0 cm to $+6.0$ cm in the horizontal axis of Fig. 2.

On-site measurements were made repeating the same procedure outlined earlier, except moving the dipole diode probe detector to a larger distance. Fig. 3 shows the signal strength (dBm) versus distance from rail center (cm)

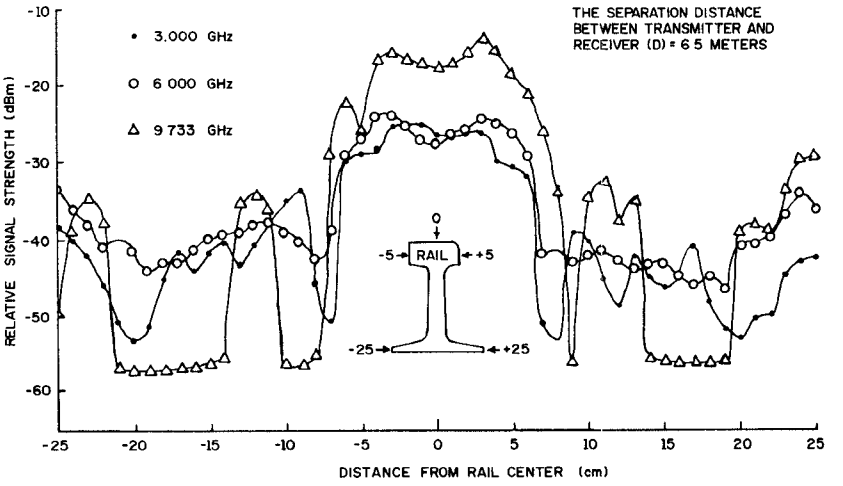

Fig. 2. The radial field strength (near field) as a function of distance from the rail top center, all the way around the rail periphery at 3.000, 6.000, and 9.733 GHz. The data show that the main part of the SEW energy (almost 90 percent) is on the head of the rails.

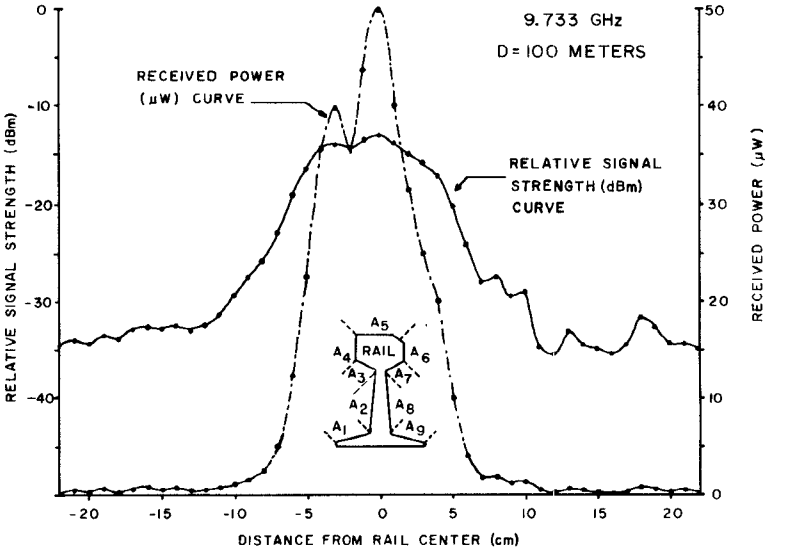

Fig. 3. Received power and radial field strength (far field) as a function of distance from the rail center around the cross section at 9.733 GHz, 100 m from the transmitting coupler and illustration of the nine areas, A_1 through A_9, used in the field strength measurements.

around the cross section at 9.733 GHz, 100 m from the transmitting coupler. The curve in Fig. 3 (far field) is smoother than that of Fig. 2 (near field). The rail was divided into 9 sections, as illustrated in the inset of Fig. 3, i.e., A_5 is the section of the flat top surface of the head, A_4 and A_6 the two sides of the head, A_3 and A_7 the bottom of the head, A_2 and A_8 the webs, A_1 and A_9 the flanges. The percentage of energy distribution on the corresponding section of the rail is calculated as

$$P_t = \sum_{i=1}^{9} P_i$$

$$\delta(A_i) = \frac{P_i}{P_t} \times 100 \quad \text{(percent)}$$

where P_t is the total power measured along the curve. P_i is the power integrated along each corresponding segment of the curve. In the equation given above, the percentage of A_i is obtained from the ratio of signal strength P_i over P_t. In fact, both P_t and P_i decrease as the distance from the signal source increases.

The signal strengths of the external field at 9.733 GHz were measured as a function of distance from the transmitting horn at 6.5, 35, 50, and 100 m, respectively. The results are summarized in Table I and show that the energy basically remains distributed in approximately the same fashion at four different distances from the source. The near field data has more of its energy on the sides of the head (as indicated by the larger $\delta(A_4+A_6)$ value and smaller $\delta(A_5)$ value) while the far field data indicates the higher percentage at the top of the head.

It is found that $\delta(A_2)$ and $\delta(A_9)$ increase with increasing distance. This could be explained by the existence of nonuniformities along the rail. Taking average percentages for four cases, the inside edge portions of rail, i.e., $\delta(A_1)$, $\delta(A_2)$, $\delta(A_3)$, and $\delta(A_4)$ are less than that of

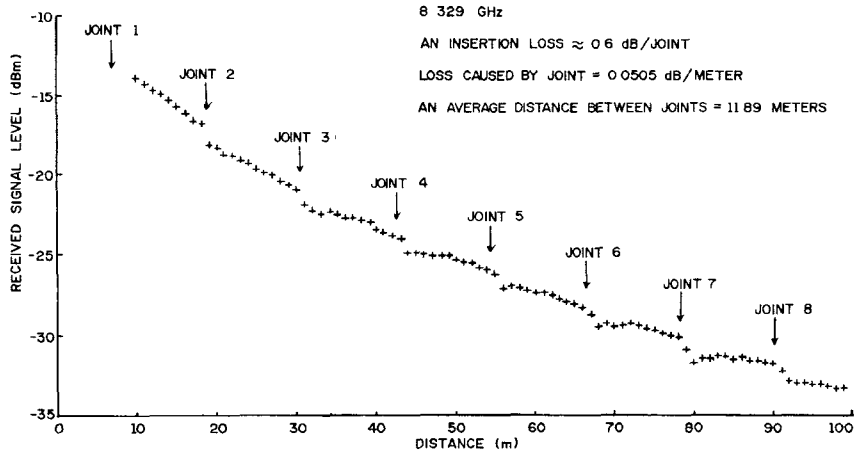

Fig. 4. Typical received signal level versus distance between couplers. This data is for a frequency of 8.329 GHz and illustrates the apparent decrease in attenuation as the receiving coupler is moved farther from the transmitting coupler (data by Brandon and Lenharth [9]).

TABLE I
ENERGY DISTRIBUTION FOR THE FLAT TOP OF HEAD, SIDE OF HEAD, BOTTOM OF HEAD, WEB, AND FLANGE AT THE DISTANCES 6.5 m, 35 m, 50 m, AND 100 m FROM THE SOURCE AT 9.733 GHz

DISTANCES FROM SOURCE d(meters)	$\delta(A_1)$ (%)	$\delta(A_2)$ (%)	$\delta(A_3)$ (%)	$\delta(A_4)$ (%)	$\delta(A_5)$ (%)	$\delta(A_6)$ (%)	$\delta(A_7)$ (%)	$\delta(A_8)$ (%)	$\delta(A_9)$ (%)	$\delta(A_4+A_5+A_6)$ (%)
65	0 3	1 7	1 2	15 8	55 6	19 2	2 2	3 9	0 1	90 6
35	0 3	1 5	2 2	15 1	59 8	15 3	2 7	3 0	0 1	90 2
50	0 3	1 0	2 4	15 1	60 1	16 2	2 1	2 2	0 6	91 4
100	0 3	2 7	1 0	9 3	64 4	17 8	1 7	1 8	1 0	91.5
AVERAGE	0 3	1 7	1 7	13 8	60 0	17 1	2 2	2 7	0 5	90 9

outer side $\delta(A_6)$, $\delta(A_7)$, $\delta(A_8)$, and $\delta(A_9)$. This was attributed to the sides of rail and joint bars being asymmetrical.

However, for each case, as illustrated in Table I, the head considered as a whole, $\delta(A_4+A_5+A_6)$, has approximately equivalent percentage of the field strength distribution greater than 90 percent for all distances.

The power received at the receiving coupler, which decouples the received SEW from the rail head shows a large decrease as a function of the measurement point from the transmitter as shown in Fig. 4 for 8.329 GHz. This figure also illustrates the effect which joints have on the propagation of a SEW. As can be seen there is an insertion loss of approximately 0.6 dB per joint. Since this loss has been included in the value obtained for the attenuation coefficient (α), it is conceivable that welded rail would have an α that is lower by 0.05 dB/m (0.6 dB loss per joint divided by the average distance of 11.89 m (39 ft) between joints on the test track). When an attenuation coefficient (α) is computed from this data, there is an apparent decrease in the attenuation coefficient as the distance between the receiving coupler and transmitting coupler is increased since the average loss per meter decreases from about 0.3 dB/m to about 0.1 dB/m over the 100-m distance with an average of about 0.2 dB/m [9].

It was found that energy of the SEW is redistributed about the rail. The energy is confined to the flat portion of the railhead near the prism coupler but that at large distances the energy is partially carried by the sides of the head, the web and the flange of the rail. This indicates that one must make attenuation measurements as far as possible down the rail line from the transmitting coupler to get reliable and accurate data. In these studies, with the limitation of a 100-mW source and our present detector–receiver system, reliable data could be obtained only out to 110 m.

B. Dielectric Strip Augmentation

The purpose of this experiment was to measure the effect that augmentation of the rail with a dielectric strip would have on the attenuation coefficient in the optimum frequency range. The detailed setup for the measurements of dielectric strip augmentation was the same as shown in Fig. 1 except that the dipole diode probe was removed and a horn antenna was used to receive the signal.

1) Thick Dielectric Augmentation of Rails: A horn-antenna prism coupler was used to launch a SEW on a rail with the configuration of Fig. 5. Here, 3-in (7.62-cm) wide strips of 1-in (2.54-cm) thick polystyrene on the side of rail were used to investigate thick dielectric augmentation in the sweep frequency range of (8–11.5) GHz. The frequency response versus field strength at 30 ft (9.144 m) from the source was plotted by an $X-Y$ recorder. For comparison, the unaugmented field strength was also plotted.

The field strength varied sinusoidally with frequency for the augmented case. The maximum received signal occured at a frequency of 8.4 GHz with lesser maxima occuring at 9.25, 9.9 and 10.7 GHz. These data indicated that an optimum frequency does exist for thick dielectric augmentation. It should be noted that these data were taken using swept frequency, so that the coupling was not as efficient as is possible for single frequency measurements where conditions may be optimized.

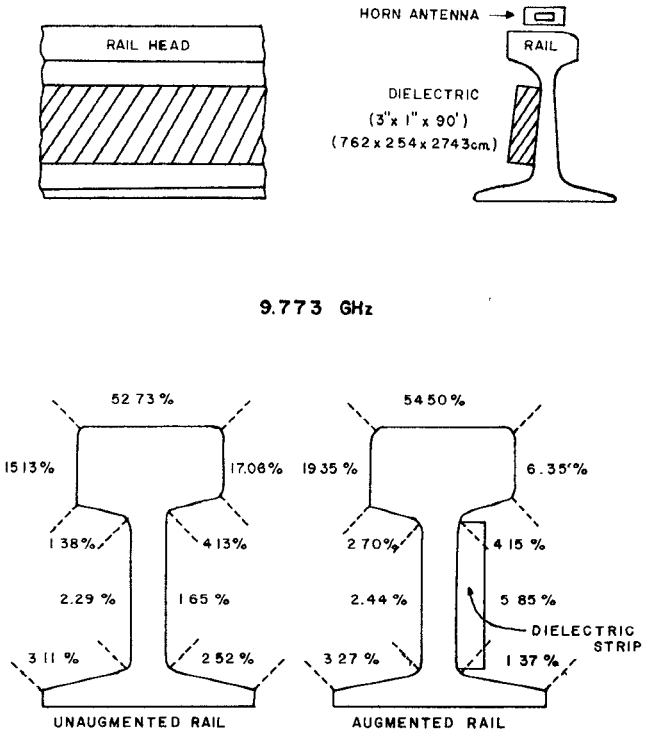

Fig. 5. Dielectric augmentation scheme for thick dielectric augmented rail and typical example for comparison of energy distribution around the rail cross section for a SEW propagating along the unaugmented rail and the augmented rail.

To investigate the effect of the dielectric augmentation on the attenuation of the SEW, the horn antennas were separated by one foot (30.48 cm) intervals between 12 ft (3.65 m) and 90 ft (27.43 m). The attenuation constant was determined by sampling the signal strength of the SEW along the rail in the direction of propagation. These data were then used to obtain values of power readings at discrete distances. The differences in level between adjacent readings were found, added together, and divided by the sum of each interval length to obtain a value for the attenuation per meter over each interval including the loss due to rail joints. This was averaged and a standard deviation was calculated. For comparison under the same conditions, the experiments were repeated with unaugmented rail.

The data for the cases with augmented and unaugmented rail with corresponding frequencies are tabulated in Table II. It is evident that in a middle band of frequencies from 8.50 to 10.50 GHz, the attenuation is lower for the thick dielectric augmented rail than for the unaugmented rail, but at frequencies both above 10.50 GHz and below 8.50 GHz the thick dielectric augmented rail has a higher attenuation. For example, the average ratio of the attenuation constants with and without dielectric augmentation over the range of 3.65–27.43 m (12–90 ft), show an increase in propagation distance (reciprocal of reduction in attenuation) which is 1.44 over the selected band from 8.25 to 11.25 GHz (0.70 standard deviation) and 1.69 over the selected band from 8.50 to 10.50 GHz (0.65 standard deviation).

TABLE II
ATTENUATION CONSTANTS WITH THICK DIELECTRIC AUGMENTATION AND WITHOUT DIELECTRIC AUGMENTATION OVER THE RANGE OF 3.65–27.43 m (12–90 ft)

FREQUENCY (GHz)	WITH DIELECTRIC (dB/m)	(NEPERS/m)	WITHOUT DIELECTRIC (dB/m)	(NEPERS/m)
8 25	0 56	0064	0 50	0057
8.625	0.34	0 039	0 51	0 058
9.00	0.44	0 051	0 46	0.052
9.25	0.27	0.031	0.57	0.065
9 50	0 32	0 037	0 46	0 052
9 773	0 28	0 032	0 82	0 094
9 858	0 21	0 024	0 47	0 054
10 00	0 43	0 049	0 54	0 062
10.125	0.43	0.049	0 43	0.049
10 25	0 43	0 049	0.38	0 043
10 375	0 38	0044	0 85	0 097
10.50	0 41	0 041	0 76	0 087
10.75	0.48	0.055	0 37	0 042
11 00	0 54	0 062	0 38	0 043
11 25	0 57	0 066	0 39	0044

For SEW propagating on rails, assuming $f = 10$ GHz, where the rail properties are conductivity $\sigma = 0.6 \times 10^8$ mho/m and relative permittivity $\epsilon_r = 1, \omega\epsilon$ becomes 0.556 and thus $\omega\epsilon \ll \sigma$. Again, for SEW propagating at the interface between rail and dielectric, the dielectric strip has relative permittivity $\epsilon_r = 1.9$ and loss tangent, $\tan \delta = 0.007$, the calculated values are $\omega\epsilon = 1.056$ and $\sigma = 0.0074$ thus, $\omega\epsilon \gg \sigma$. Schelkunoff [11] suggests that most surface waves can be explained by either trapped surface waves or surface waves due to lossy surfaces. The former occurs for $\omega\epsilon \gg \sigma$ in which a wave propagates in a given direction by repeated back and forth reflection between two interfaces.

McAulay [10] has made theoretical studies using the finite element method of analysis of SEW on complicated shaped structures, involving augmentation of the rail by means of dielectric material so that a surface wave is held close to the metallic surface region. The surface wave is enhanced internal reflection as the wave propagates. The recommendation resulting from his theoretical study was that the entire area of the web from the flange to head be filled with dielectric.

2) Field Strength Distribution of Dielectric Augmented Rails: The energy distribution percentages for the augmented rail's field strength vs the unaugmented rail's field strength (shown in Fig. 5) were determined by a dipole diode probe receiver as shown in Fig. 1. The results show that more energy is held in the portion of the rail which contains dielectric than was present on the unaugmented rail.

The field strength is apparently enhanced on the web of the rail with augmentation because a portion of the surface wave may be trapped inside the dielectric strips by repeated reflection as the wave propagates.

C. Intertrack Coupling

Measurements of intertrack coupling were made using both the horn detector and the probe detector in the 4–8-GHz, 8–12-GHz, and 12–18-GHz frequency bands.

The signal level was measured as a function of distance from the transmitting horn on both the signal guiding rail and the adjacent rail at the on-site rail tracks. The received signals were measured at 5-m intervals on both rails, starting 20 m from the transmitter prism. The signal on the adjacent rail (intertrack coupling signal) was at all times below the minimum detectable signal level (−50 dBm), verifying that there is no intertrack coupling in the 4–18-GHz frequency range.

III. Discussion and Conclusions

More than 90 percent of SEW energy on rail tracks is on the top and sides of the head of the rail as detected by a dipole diode probe detector. The apparent large attenuation coefficient measured at short distances from the transmitting coupler is probably caused by the redistribution of the SEW and does not constitude a "real" loss of energy. It is important to note, in connection with the obstacle insertion loss data [9], that a blockage of the top of the rail causes the SEW energy to redistribute itself to the lower portion of the rail at the blockage and, in a short distance past the blockage, the energy then redistributes back to the top of the rail.

It is desirable that a Railway Collision Avoidance System detect vehicles at large distances (500 to 1000 m for Urban Commuter Systems). Since the apparent attenuation of the signal is a function of distance from the transmitter, estimates of the anticipated propagation distances cannot be made merely from the near field attenuation measurements but the far field data must be used because of the decrease in attenuation with distance.

It was found that the signal on the adjacent rail was below the minimum detectable signal level, which indicates that there is no measurable intertract coupling in the 4–18-GHz frequency range. For the thick dielectric augmented rail the frequency response vs field strength at 30 ft (9.144 m) from the source indicates that field strength varied sinusoidally with frequency, exhibiting maxima approximately 0.8 GHz apart. The field strength at the same frequencies is found to be apparently enhanced on the rail with dielectric augmentation. The average increase in propagation distance is 1.44 over the selected band from 8.25 to 11.25 GHz and 1.69 over the selected band from 8.5 to 10.5 GHz.

For 5-kW pulse capability, applying the multiplication factor of 1.69 available with thick dielectrics to the measured attenuation coefficients predicts an increase in propagation distance from 799 m for the presently existing unimproved systems [9] up to 2179 m for improved systems. Use of dielectric augmentation clearly can increase the range of a SEW Collision Avoidance System but it should be realized that it would also increase the cost.

The increase in propagation distance, although large, is not as large as predicted by McAulay's [10] theoretical work and occurs at different frequencies than those predicted. This is attributed in part to the fact that the dielectric slabs used in these experiments did not completely fill the web from the flange to the head.

For any practical SEW system utilized in a railway application, an experimental knowledge of the electromagnetic field distribution and propagation characteristic is essential. The data presented clearly indicate that the field strength of the SEW propagating on the rail can be enhanced by proper selection of dielectric augmentation and excitation frequency.

Acknowledgment

The authors wish to thank B. Lenharth and D. Brandon, whose help is gratefully acknowledged, as are many stimulating discussions with D. Begley. The authors are also grateful to the St. Louis–San Francisco Railway Company, who kindly gave permission to conduct experimental tests on their railroad tracks.

References

[1] T. Kawakami, T. Maruhama, T. Takeya, and S. Kohno, "Waveguide communications system for centralized railway traffic control," *IEEE Trans. Vehicular Commun.*, vol. vc-13, pp. 1–17, Sept. 1964.

[2] H. M. Barlow, "High frequency guided electromagnetic waves in application to railway signalling and control," *Radio Electron. Eng.*, vol. 33, pp. 275–281, May 1967.

[3] Y. Amemiya, N. Kurits, T. Nakahara, N. Kurauchi, and T. Nagao, "Surface wave radar system," *Sumitomo Elec. Tech. Reb.*, vol. 3, pp. 49–56, 1964.

[4] Y. Amemiya, N. Kurits, T. Nakahara, N. Kurauchi, and T. Nagao, "Surface waveguides for railway application," in *Proc. Int. Conf. Microwaves, Circuit Theory, Inform. Theory*, (Tokyo, Japan) 1964, Pt. 3, pp. 15, MI-8, Inst. Electron. Commun. Japan, 1964.

[5] H. H. Ogilvy, "Radar on the railways," *Electron. Power (J. IEE)*, vol. 10, pp. 146–150, May 1964.

[6] M. Davarpanah, "Excitation of surface electromagnetic waves at microwave frequencies using optical techniques," Ph.D. dissertation, Univ. Missouri-Rolla Library, Rolla, 1975.

[7] M. Davarpanah, C. A. Goben, D. L. Begley, and S. L. Griffith, "Surface electromagnetic wave coupling efficiencies for several excitation techniques," *Appl. Opt.*, vol. 15, p. 3066, Dec. 1976.

[8] M. Davarpanah, C. A. Goben, and R. J. Bell, "Excitation efficiency of surface electromagnetic waves using prism and grating coupling techniques," *Wave Electron.*, vol. 3, p. 19, 1977.

[9] C. A. Goben and M. Davarpanah, "The excitation and propagation of surface electromagnetic waves on a railroad rail with applications to collision avoidance," Final Rep. DOT-TSC-UMTA-76-12 for the U.S. Dep. Transportation, Transportation Systems Center, Cambridge, MA, Oct. 1977.

[10] A. D. McAulay, "Variation finite-element solution for dissipative waveguides and transportation application," *IEEE Trans. Microwave Theory Tech.*, vol. MTT-25, pp. 382–392, May 1977.

[11] S. A. Schelkunoff, "Anatomy of surface waves," *IRE Trans. Antennas Propagat*, (Symposium), pp. S133, 1959.